Deletion of G protein-coupled receptor 48 leads to ocular anterior segment dysgenesis (ASD) through down-regulation of Pitx2

Jinsheng Weng*, Jian Luo*†, Xuhong Cheng*, Chang Jin‡, Xiangtian Zhou‡, Jia Qu‡, LiLi Tu‡, Di Ai*, Dali Li*†, Jun Wang*, James F. Martin*, Brad A. Amendt*, and Mingyao Liu*†‡§

*Institute of Biosciences and Technology and Department of Molecular and Cellular Medicine, Texas A&M University System Health Science Center, 2121 West Holcombe Boulevard, Houston, TX 77030; †Institute of Biomedical Sciences and School of Life Sciences, East China Normal University, Shanghai 200241, China; and ‡School of Optometry and Ophthalmology and Eye Hospital, Wenzhou Medical College; Key Laboratory Cultivation Base and Key Laboratory of Vision Science, Ministry of Health P.R. China and Zhejiang Provincial Key Laboratory of Ophthalmology and Optometry, 270 Xueyuan Road, Wenzhou, Zhejiang 325003, China

Edited by Melvin I. Simon, California Institute of Technology, Pasadena, CA, and approved February 11, 2008 (received for review August 31, 2007)

The development of the anterior segment of the mammalian eye is critical for normal ocular function, whereas abnormal development can cause glaucoma, a leading cause of blindness in the world. We report that orphan G protein-coupled receptor 48 (Gpr48/LGR4) plays an important role in the development of the anterior segment structure. Disruption of *Gpr48* causes a wide spectrum of anterior segment dysgenesis (ASD), including microphthalmia, iris hypoplasia, irdiocorneal angle malformation, cornea dysgenesis, and cataract. Detailed analyses reveal that defective iris myogenesis and ocular extracellular matrix homeostasis are detected at early postnatal stages of eye development, whereas ganglion cell loss, inner nuclear layer thinness, and early onset of glaucoma were detected in 6-month-old *Gpr48*$^{-/-}$ mice. To determine the molecular mechanism of ASD caused by the deletion of *Gpr48*, we performed gene expression analyses and revealed dramatic down-regulation of *Pitx2* in homozygous knockout mice. *In vitro* studies with the constitutively active Gpr48 mutant receptor demonstrate that Pitx2 is a direct target of the Gpr48-mediated cAMP-CREB signaling pathway in regulating anterior segment development, suggesting a role of Gpr48 as a potential therapeutic target of ASD.

eye development | glaucoma | cataract | Lgr4

The function of the vertebrate retina, which transduces light into electrical signals to the brain, depends on a considerable number of highly differentiated tissues in the anterior eye segment. Cornea and lens provide transparency and refraction, the iris protects the retina from excess exposure of light, and the ciliary body (CB) secretes aqueous humor that flows between the lens and the anterior chamber to provide nutritional needs for the lens and cornea. Malformation of the anterior structures in the eye can dramatically affect vision function and blockage of aqueous humor outflow, leading to the increase of intraocular pressure (IOP) (1, 2). Chronic IOP is an important risk factor for glaucoma, a leading blindness disease in the world, affecting ≈70 million individuals (3).

G protein-coupled receptors (GPCRs) play key roles in a variety of physiological functions. Gpr48, also called LGR4, belongs to the leucine-rich GPCR (LGR) family (4–6). Members of this family have multiple leucine-rich repeats at the N terminus and a seven-transmembrane domain (7). Many studies suggest that the expanding family of LGRs, including three known glycoprotein hormone receptors (LH, FSH, and TSH), the orphan receptor LGR4 (Gpr48)-LGR6, and LGR7–8, are homologous and conservative (4–7). The mammalian glycoprotein hormone receptors have diverse structural features and mainly couple through the cAMP-dependent pathway for signal transduction (4–6). Gpr48 is widely expressed in multiple organs at both the embryonic and adult stages (8, 9), suggesting a vital role in development and adult physiological functions. Recent studies demonstrate that Gpr48/LGR4 plays important roles in growth retardation and renal and reproductive system development (9–11). Furthermore, up-regulation of Gpr48 promotes carcinoma cell invasion and metastasis (12). However, so far little is known about the function and molecular mechanism of Gpr48 in eye development and dysgenesis.

To understand the biological function of Gpr48, we have generated *Gpr48*-null mice by using the gene-trap technique and examined the expression of Gpr48 in eye [see supporting information (SI) Figs. S1 and S2 and *SI Text*). We demonstrate that *Gpr48*-null mice have a spectrum of anomalies in the anterior segment of the eye, including microphthalmia, iris hypoplasia, irdiocorneal angle malformation, cornea dysgenesis, and cataract. At early stages of eye development, we found that *Gpr48*$^{-/-}$ homozygous mutant mice have decreased iris myogenesis and defective extracellular matrix homeostasis. Detailed study of the expression levels of different transcription factors demonstrates that *Pitx2* is dramatically down-regulated in *Gpr48*-null mutant mice. We further demonstrate that Gpr48 can increase the intracellular cAMP level, which activates cAMP-dependent PKA and directly regulates *Pitx2* expression through CREB transcription factor binding to the *Pitx2* promoter. Together, our studies demonstrate that Gpr48 regulates ocular anterior segment development. Disruption of Gpr48 function can lead to anterior segment dysgenesis (ASD) through down-regulation of Pitx2, a key transcription factor in anterior segment development (13–15), suggesting Gpr48 as a potential therapeutic target of ASD.

Results

***Gpr48* Disruption Induces Microphthalmia, Iris Hypoplasia, and Iridiocorneal Abnormality.** To explore the biological function of Gpr48 *in vivo*, we generated *Gpr48* homozygous mutant mice (*Gpr48*$^{-/-}$ mice) by microinjecting gene trap-mutated *Gpr48* ES cells into blastocysts of C57BL/6 mice. The *Gpr48*$^{-/-}$ mice demonstrated growth retardation in the embryo and postnatal day 0 (P0) mice, and their weight was ≈60–70% of their wild-type littermates. *Gpr48*$^{-/-}$ mice show a perinatal death phenotype, and ≈60% of newborn homozygous mice die around P0 and day 1, which is consistent with previous reports (9). Although the mortality of *Gpr48*$^{-/-}$ mice is high at P0 and day 1, the mortality of mutant mice is decreased significantly after day 1. Of 47 adult *Gpr48*$^{-/-}$ mice that

Author contributions: J. Weng and M.L. designed research; J. Weng, J.L., X.C., C.J., X.Z., D.A., D.L., and J. Wang performed research; J.Q., L.T., J.F.M., and B.A.A. contributed new reagents/analytic tools; J. Weng and M.L. analyzed data; and J. Weng and M.L. wrote the paper.

The authors declare no conflict of interest.

This article is a PNAS Direct Submission.

§To whom correspondence should be addressed. E-mail: mliu@ibt.tamhsc.edu.

This article contains supporting information online at www.pnas.org/cgi/content/full/0708257105/DCSupplemental.

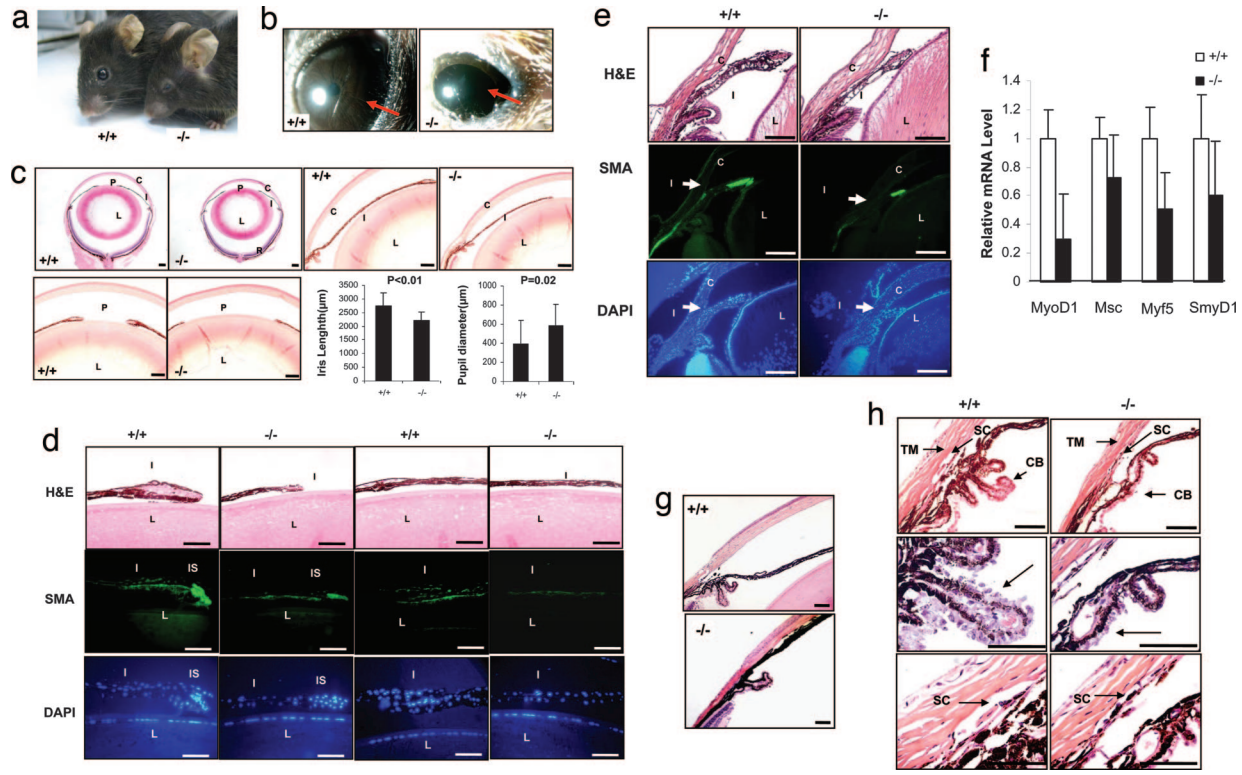

Fig. 1. Microphthalmia, iris hypoplasia, and iridiocorneal abnormality in *Gpr48*$^{-/-}$ mice. (*a*) Microphthalmia in *Gpr48*$^{-/-}$ mice. (*b*) Iris hypoplasia demonstrated by Slit lamp examination of adult mice. *Gpr48*$^{-/-}$ mice have hypoplasia of the iris with a larger pupil (arrows) relative to wild-type mice under strong light exposure. (*c*) Midsagittal sections of the entire eye showing short iris and bigger pupil in *Gpr48*$^{-/-}$ (−/−) compared with wild-type mice (+/+). Detailed analysis of 24 *Gpr48*$^{-/-}$ and wild-type mice indicates the iris length is significantly shorter, whereas the pupil size is much bigger in *Gpr48*$^{-/-}$ compared with wild-type mice. (*d*) Smooth muscle hypoplasia and reduction in cell numbers in the iris of *Gpr48*$^{-/-}$ mice. The pupil part of iris in *Gpr48*$^{-/-}$ mice is much smaller than in wild type. The middle part of the iris in *Gpr48*$^{-/-}$ mice is much thinner than in wild type (H&E staining). The stroma portion in the *Gpr48*$^{-/-}$ iris can hardly be detected. SMA staining of the iris smooth muscle cell in adult mice demonstrates a decrease of SMA in both the pupil and the middle portions of iris muscle cells in *Gpr48*$^{-/-}$ mice (SMA staining). DAPI staining indicates that the number of cells was significantly reduced in both the stroma and the middle portion of the iris in *Gpr48*$^{-/-}$ mice (DAPI). (*e*) Iris myogenesis in postnatal day 4 *Gpr48*$^{-/-}$ mice. H&E staining shows that the iris is short and small in postnatal day 4 *Gpr48*$^{-/-}$ compared with wild-type mice. SMA immunofluorescence staining is weak in *Gpr48*$^{-/-}$ compared with wild-type mice. (*f*) The expression levels of key genes in myogenesis, including *Mf5*, *Smy1D1*, *MyoD1*, and *Msc*, were significantly decreased in P0 *Gpr48*$^{-/-}$ mice. (*g*) Iris–cornea adhesion and close of iridocorneal angle were detected in *Gpr48*$^{-/-}$ mice. (*h*) Iridocorneal structure anomalies in *Gpr48*$^{-/-}$ mice. The CB of *Gpr48*$^{-/-}$ mice contains less folding and fewer cells in the outer layer of the CB. The TM is compressed in *Gpr48*$^{-/-}$ compared with wild-type mice. *C*, cornea; I, iris; L, lens; P, pupil; R, retina. [Scale bars: 170 μm (*c*), 43 μm (*d*), and 85 μm (*e*–*h*).]

survived, there are 20 *Gpr48*$^{-/-}$ male and 27 *Gpr48*$^{-/-}$ female mice. Initial examination shows that 15 of 20 *Gpr48*$^{-/-}$ male mice (75%) showed a small eye phenotype (microphthalmia), and 10 of 27 female mice have a small eye phenotype (37%) (Fig. 1*a*).

Because the small eye phenotype is frequently associated with iris hypoplasia and the expression of *Gpr48* in the iris stroma, we further examined whether *Gpr48*$^{-/-}$ mice have iris hypoplasia using Slit Lamp assays. When exposed to strong light, the iris of the wild-type mice expanded and formed a dark-brown layer in front of the lens to prevent too much light from entering the eyes. However, in *Gpr48*$^{-/-}$ mice, a dark-brown layer was not formed, and only a small layer of brown tissue can be detected at the rim of the cornea, indicating that *Gpr48*$^{-/-}$ mice have iris hypoplasia (Fig. 1*b*). Upon close histological examination, we found that the iris in *Gpr48*$^{-/-}$ mice was much shorter and thinner than in wild-type mice (Fig. 1*c*). The pupil diameter is significantly increased in *Gpr48*$^{-/-}$ mice (Fig. 1*c*). Histology analysis also revealed that the stroma portion of the iris is dramatically reduced in the *Gpr48*$^{-/-}$ mice (Fig. 1*d*, H&E staining). In the pupil portion of the wild-type iris, the stroma part is large, with a large number of stroma cells (25–35 cells per pupil iris, DAPI staining). In *Gpr48*$^{-/-}$ mice, however, the size of the iris stroma is small, with decreased stroma cells (12–18 cells per pupil iris, Fig. S3*d*, DAPI staining). The total thickness in the middle part of the iris stroma is also dramatically reduced in *Gpr48*$^{-/-}$ mice (Fig. 1*d Right*). Because the iris stroma contains smooth muscle cells, we further examined whether iris smooth muscle was hypoplasic in *Gpr48*$^{-/-}$ mice using smooth-muscle actin (SMA) immunofluorescence staining. We found that the staining of SMA was dramatically weaker in *Gpr48*$^{-/-}$ compared with wild-type mice (Fig. 1*d*, SMA staining), suggesting that deletion of *Gpr48* in mice induces iris smooth muscle hypoplasia. In P4 mice, we found similar reduced SMA immunofluorescence staining in *Gpr48*$^{-/-}$ mice (Fig. 1*e*), indicating that early iris muscle development was defective in *Gpr48*$^{-/-}$ mice. These data are further confirmed by the down-regulated expression of *MyoD1*, *Mf5*, *Msc*, and *Smy1D* in P0 *Gpr48*$^{-/-}$ mice (Fig. 1*f*). Although the degree of iris hypoplasia varies from mouse to mouse, all *Gpr48*$^{-/-}$ mice we examined have iris hypoplasia.

Iridocorneal structure malformation was found in all *Gpr48*$^{-/-}$ mice with different degrees of defects (Fig. 1g, Fig. S4, and Table S1). The iridocorneal angle is smaller in *Gpr48*$^{-/-}$ mice. In extreme cases (3 of 24 *Gpr48*$^{-/-}$ mice), the corneal angle was totally closed because of the adhesion of the iris with the cornea (Fig. 1*g*). The CB is much smaller in all *Gpr48*$^{-/-}$ mice compared with wild type (Fig. 1*h*), containing less folding and fewer cells in the folding (Fig. 1*h*, middle arrow). The trabecular meshworks (TM) in *Gpr48*$^{-/-}$ mice are also compressed and contain many fewer trabecular beams with

smaller beam size than those in wild-type mice. Schlemm's canal (SC) was much smaller in both length and width (Fig. 1*h Bottom*).

Keratopathy and Cornea Dysgenesis in *Gpr48*$^{-/-}$ Mice. Careful examination of *Gpr48*$^{-/-}$ mouse eyes reveals that ≈40% (18 of 47) of the mutant mice also have cornea opacity. A cloudy white nontransparent structure formed in the center or around the rim of the cornea (Fig. S3*a*). Most of these mice (15 of 18) also have cornea neovascularization (Fig. S3*a*). Histological analyses reveal that other keratopathies also exist, including cornea inflammation and neovasculization (Fig. 3*b* IF, 10%, 5 of 47); cornea epithelial plug (Fig. S3*b*, ≈16%, 8 of 47); cornea vascular pannus (Fig. S3*b*, 8%, 4 of 47); cornea cystic-like lesion (Fig. S3*b*, 10%, 5 of 47), and loss of surface smoothness (Fig. S3*b*, 8%, 4 of 47). The appearance of keratopathy was more frequently found in male and old *Gpr48*$^{-/-}$ mice than in female and young mice, indicating that the protective function of the cornea epithelium is compromised in *Gpr48* mutant mice.

To evaluate whether the cornea epithelium has a developmental defect, we examined cornea epithelium morphology at both the early postnatal periods and in adult mice (Fig. S3*c*). At day 0, both mutant and wild-type mice have one to two layers of cornea epithelial cells, and the cornea stroma is not different from that in wild-type mice. Beginning at P10, however, the cornea epithelium layers of mutant mice become significantly thinner than in wild type (Fig. S3*c*, P10 and P14). H&E staining demonstrates that cells in the mutant cornea appear shrunken and more compact compared in wild-type mice (Fig. S3*c*, P10 and P14). These changes in the cornea epithelium continue in adult mice (Fig. 3*c*, 2M). Further studies of the cornea epithelium demonstrate that both cell proliferation [Fig. S3*d*, proliferating cell nuclear antigen (PCNA)] and cell differentiation (Fig. 3*d*, K12) are decreased in *Gpr48*-null mutant mice, as demonstrated by marker staining. Besides cornea epithelium thinness, the cornea stroma of adult *Gpr48*$^{-/-}$ mice is also significantly thinner than in wild type (Fig. S3*e*).

To see whether the structure of the collagen fibers was normal in mutant mice, we performed electronic microscopic analysis of *Gpr48*-null mutant mice. We found that the lamellar arrangement of collagen in the mutant cornea was seriously disturbed in *Gpr48*-null mutant mice (Fig. S3*f*). The cornea fibrils cross each other randomly and leave significant portions of electron lucent space in the cornea stroma of *Gpr48*$^{-/-}$ mice (Fig. S3*f*). In wild type, however, collagen fibrils are arranged in a regular lamellar structure, crossing each other at right angles and forming a highly ordered 3D structure in the cornea (Fig. S3*f Left*).

The expression levels of key extracellular matrix proteins, including collagen I, collagen V, biglycan (BGN), osteoglycan (OGN), keraton, decorin (Den), and lumican were decreased in newborn *Gpr48*$^{-/-}$ mouse eyes (Fig. S3*g*). PLOD1 and PLOD2, two key enzymes that regulate collagen homeostasis (16), are also decreased in *Gpr48*$^{-/-}$ mice, as measured by real-time PCR analysis in newborn mouse eyes (Fig. S3*h*), suggesting the disruption of the extracellular matrix protein homeostasis in the cornea of *Gpr48*$^{-/-}$ mice.

Cataract and Early Onset of Glaucoma in *Gpr48*$^{-/-}$ Mice. We found that ≈26% (13 of 47) of *Gpr48*$^{-/-}$ mutant mice have cataracts by using the Slit Lamp test (Fig. 2*a*). The white nontransparent structure located in the lens of *Gpr48*$^{-/-}$ mice was detected (Fig. 2*a*). Lens opacity ranged from total (Fig. 2*a*, TL) to partial lens opacity (Fig. 2*a*, PL). Some mutant mice have both opaque lenses associated with iris-corneal adhesion (Fig. 2*a*, arrow). Upon histological analysis, we found that mutant lens fibers are disorganized and abnormally larger in the cortical zone of lens in *Gpr48*$^{-/-}$ mice with cataract (Fig. 2*b*). Abnormal protein deposits are detected in some lens cells (Fig. 2*b*, arrow). In those mutant mice that do not have apparent lens fiber anomalies, the lens diameter was significantly reduced (Fig. 2*c*) ($P = 0.02$). Because αA-crystallin is the major protein in the lens, we examined the expression level of αA-crystallin by Western blot analysis with equal weight of lens. We found that the ratio of soluble and insoluble αA-crystallin was significantly different between wild-type and mutant *Gpr48*$^{-/-}$ mice (Fig. 2*d*). A large amount of insoluble protein can be detected in mutant but not in wild-type mice (Fig. 2*d*, insoluble), which could explain the abnormal protein deposits in the mutant mouse lens. Further analysis reveals that the promoter of αA-crystallin can be directly activated by cotransfection of *Gpr48* constitutively active mutant receptor in the cells (Fig. 2*e*), suggesting that αA-crystallin is a direct downstream target regulated by Gpr48 activation.

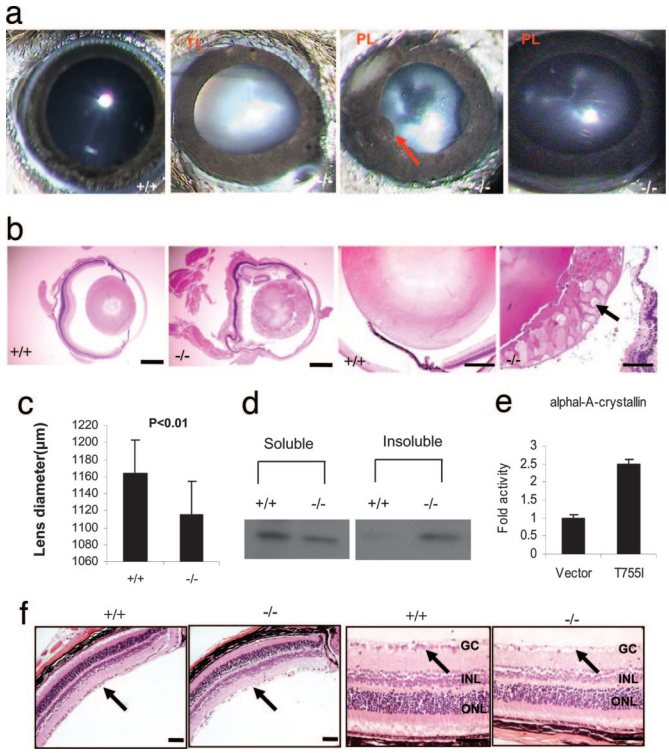

Fig. 2. Cataract and ganglion cell loss in *Gpr48*$^{-/-}$ mice. (*a*) Lens opacity in *Gpr48*$^{-/-}$ mice. Total and partial lens opacity and iris cornea adhesion are detected in *Gpr48*$^{-/-}$ mice. (*b*) Histological analysis shows abnormal lens fibers in the lens cortical zone of *Gpr48*$^{-/-}$ mice. Abnormal protein deposit is also detected (arrow) (32). (*c*) Statistical analysis shows *Gpr48*$^{-/-}$ have smaller lens compared with wild-type mice. (*d*) The ratio of soluble and insoluble αA-crystallin has been changed in *Gpr48*$^{-/-}$ mice with significant increase of insoluble αA-crystallin in *Gpr48*$^{-/-}$ mice. (*e*) Activation of αA-crystallin promoter reporter by Gpr48 active mutant T755I. (*f*) Ganglion cells loss and thinning of inner and outer nuclear layers in *Gpr48*$^{-/-}$ mice at 6 months. [Scale bars: 340 μm (*b*) and 100 μm (*f*).]

To determine whether deletion of *Gpr48* induces early onset of glaucoma, we examined the morphology changes of the retinas of *Gpr48*$^{-/-}$ and wild-type mice. The retinas from *Gpr48*$^{-/-}$ mice younger than 6 months seem normal. However, in 10 of 24 *Gpr48* $^{-/-}$ mice older than 6 months, we detected significant loss of ganglion cells and thinness and disarrangement of inner and outer nuclear cell layers, respectively (Fig. 2*f*), suggesting that Gpr48 could play an important role in the early onset of glaucoma.

Down-Regulation of the Key Transcription Factor, Pitx2, in *Gpr48*$^{-/-}$ Mice. To determine how *Gpr48* deficiency causes anterior segment structure changes, we analyzed the expression levels of transcription factors important for eye development with P0 mouse eyes. As shown in Fig. 3*a*, the expression levels of *Foxc1*, *Foxc2*, *Foxe3*, *Lmx1b1*, and *Pax6* are not changed (Fig. 3*a*), nor are *Pitx3*, *Bmp4*, *Atf4*, *Mitf*, *C-myb*, *Prox-1*, *Eya-1*, and *Sox2* in the eyes of *Gpr48*$^{-/-}$

DEVELOPMENTAL BIOLOGY

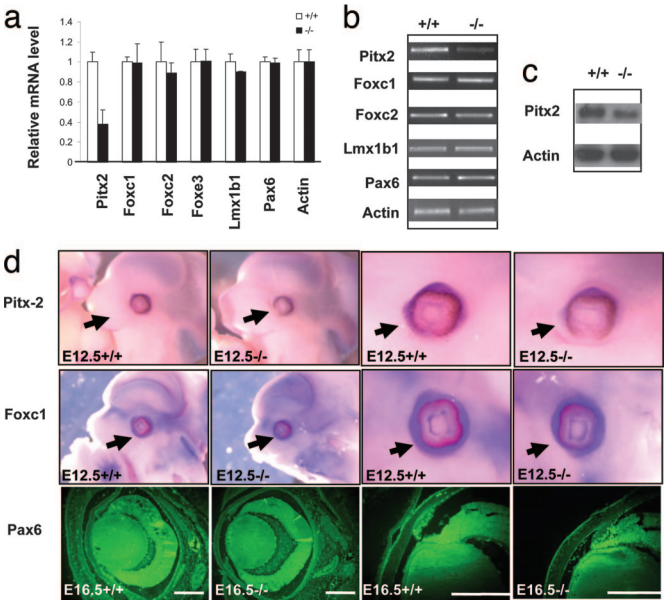

Fig. 3. Expression changes of key transcription factors in *Gpr48*$^{-/-}$ mouse eyes. (*a*) Real-time PCR analysis of transcription factors involved in ocular anterior development shows that Pitx2 is down-regulated in P0 *Gpr48*$^{-/-}$ mice. The expression levels of *Foxc1*, *Foxc2*, *Foxe3*, *Lmx1b1*, and *Pax6* are not changed. (*b*) The expression levels of transcription factors, including *Pitx2*, *Foxc1*, *Foxc2*, *Foxe3*, *Lmx1b1*, and *Pax6*, were confirmed by RT-PCR, showing decreased expression of *Pitx2* in the E12.5 *Gpr48*$^{-/-}$ embryo. (*c*) Decreased expression of Pitx2 protein using Western blot analysis with the E12.5-day embryo in *Gpr48*$^{-/-}$ mice. (*d*) Whole-mount *in situ* hybridization (*Pitx2* and *Foxc1*) and immunofluorescence staining (Pax6) in the E12.5 embryo demonstrates that *Pitx2*, but not *Foxc1* and Pax6, was significantly decreased in the *Gpr48*$^{-/-}$ embryo. [Scale bars: 85 μm (*b*).]

mice (data not shown). However, the expression level of *Pitx2* is significantly down-regulated in *Gpr48*$^{-/-}$ mice (Fig. 3*a*). The significant down-regulation of the *Pitx2* gene and Pitx2 protein was further confirmed by RT-PCR (Fig. 3*b*), *in situ* hybridization assays with *Pitx2* probes (Fig. 3*d*), and Western blot analysis, with the specific anti-Pitx2 antibody (Fig. 3*c*), suggesting that Pitx2 is a potential downstream target gene regulated by Gpr48. As controls, the expression levels of Foxc1 and Pax6 are not changed in *Gpr48*$^{-/-}$ mice in our *in situ* hybridization assays and immunofluorescence staining (Fig. 3*d*). Together, our data demonstrate that deletion of *Gpr48* significantly decreases the expression level of Pitx2, a key transcription factor in anterior segment development of the eyes.

Gpr48 Mediates the cAMP-PKA and CREB Signaling Pathway. To examine the downstream signaling pathways mediated by Gpr48, we generated six mutant receptors, four in the transmembrane domain V and VI regions (D736G, T755I, T755L, and I758G) and two mutants in the third intracellular loop (H748V and A750V) of the wild-type Gpr48 receptor (data not shown). After transfecting these mutant receptors into 293T cells, we measured the production of intracellular cAMP and found that one of the mutants, T755I, could significantly increase the intracellular cAMP level compared with cells transfected with the wild-type Gpr48 receptor and the control vector (Fig. 4*a*), consistent with the data published previously (17). The activation of the cAMP pathway was also confirmed by the activation of the CREB luciferase reporter assay in cells cotransfected with the T755I mutant receptor (Fig. 4*b*), suggesting that Gpr48 activates Gαs and adenylate cyclase to produce intracellular cAMP, which activates the CREB transcription factor (Fig. 4*b*).

Gpr48 Regulates Pitx2 Expression Through the CREB Transcription Factor and the CRE-Binding Site of the *Pitx2* Promoter. To understand the molecular mechanisms of reduced Pitx2 expression in *Gpr48*$^{-/-}$ mice, we examined $\approx$2 kb of the *Pitx2* promoter region from both human and mouse *Pitx2* genes using online computer software TESS (www.cbil.upenn.edu/cgi-bin/tess/tess). A consensus *CRE* site TGACGTCA for potential binding by the CREB transcription factor was identified at position -79 relative to the transcription start site of *Pitx2* in both species (Fig. 4*c*). To determine whether this site was important for the activation of the *Pitx2* promoter by Gpr48, we constructed different *Pitx2*-luciferase reporter genes with or without the CRE-binding site (Fig. 4*c*). We measured luciferase activity in cells transfected with the reporter genes and the *Gpr48* wild-type or active mutant (T755I) receptor, respectively. As shown in Fig. 4*d*, the active mutant of Gpr48 can activate the *Pitx2*-108-luc reporter that contains the CRE site but not the *Pitx2*-67-luc reporter in which the CRE-binding site was deleted (Fig. 4*d*). This activation is also diminished by point mutation of the CRE-binding site (from TGACGTCA to TGAAATCA) (Fig. 4*e*), indicating that the *CRE*-binding site is essential for activation of the *Pitx2* promoter by Gpr48 activation (Fig. 4*e*). Furthermore, we demonstrated that activation of the *Pitx2* promoter by Gpr48 is through a cAMP-dependent protein kinase (PKA) signaling pathway, because both competitive PKA inhibitors, PKI and H-89, can successfully inhibit the activation of the *Pitx2*-luciferase promoter mediated by the Gpr48 active mutant receptor (Fig. 4 *f* and *g*).

To further confirm that Gpr48 activate the *Pitx2* promoter via the cAMP-CREB signaling pathway, we examined the interaction of CREB with the *Pitx2* promoter using EMSA and ChIP assays. As shown in Fig. 4*h*, nuclear extracts from mouse pituitary cell αT3–1 form a binding complex with the [γ^{32}-P]-labeled *Pitx2-CRE* probe (spanning sequence from -99 to -69 in the promoter region of the mouse *Pitx2*) (Fig. 4*h*, lane 2, arrow). This band was not supershifted by nonspecific IgG and mutant probes (Fig. 4*h*, lanes 4 and 5) but was supershifted by the specific anti-CREB1 antibody (Fig. 4*h*, lane 6) and blocked by the 200-fold cold competitor probe (Fig. 4*h*, lane 3), suggesting specific binding of the CREB transcription factor to the *Pitx2* promoter. In the ChIP assay, we further found that the specific CREB antibody was capable of immunoprecipitating the *Pitx2* promoter fragment containing the CRE sites (Fig. 4*i*, lane 3) but not by the anti-IgG antibody (Fig. 4*i*, lane 2). Together, our data demonstrate that Gpr48 can regulate *Pitx2* gene expression through the cAMP-PKA-CREB signaling pathway, and that the CRE-binding site (-9) in the promoter region of *Pitx2* is essential for the regulation of Gpr48 activation (Fig. 4*j*).

Discussion

The findings presented here demonstrate that Gpr48 regulates the development of the anterior chamber of the mouse eye. Deficiency of Gpr48 resulted in a spectrum of ASD, including iris hypoplasia, iridocorneal angel malformation, corneal dysgenesis, and cataract. Detail analysis of the anterior segment of the eyes at early stages of development reveals significant defects in iris myogenesis, in cornea epithelial cell proliferation and differentiation, and in the synthesis of extracellular matrix molecules in *Gpr48*$^{-/-}$ mice. All of these defects have led to ASD in adult mice. To understand the molecular mechanisms of Gpr48-mediated ASD, we found that Pitx2 was significantly down-regulated in *Gpr48*-null mutant mice, and Pitx2 is a direct target of Gpr48 through cAMP-PKA and CREB signaling pathways. Therefore, deletion of *Gpr48* results in ASD through decreased Pitx2 expression, a key transcription factor in anterior segment development (18).

Gpr48-null mutant mice have iris hypoplasia, as demonstrated by the Slit Lamp assay. Histological analysis demonstrated that the early stage of iris muscle development in the *Gpr48*$^{-/-}$ mouse was significantly affected with diminished expression of SMA and the down-regulation of myogenesis biomarkers and transcription factors. The iris smooth muscle in the iris stroma

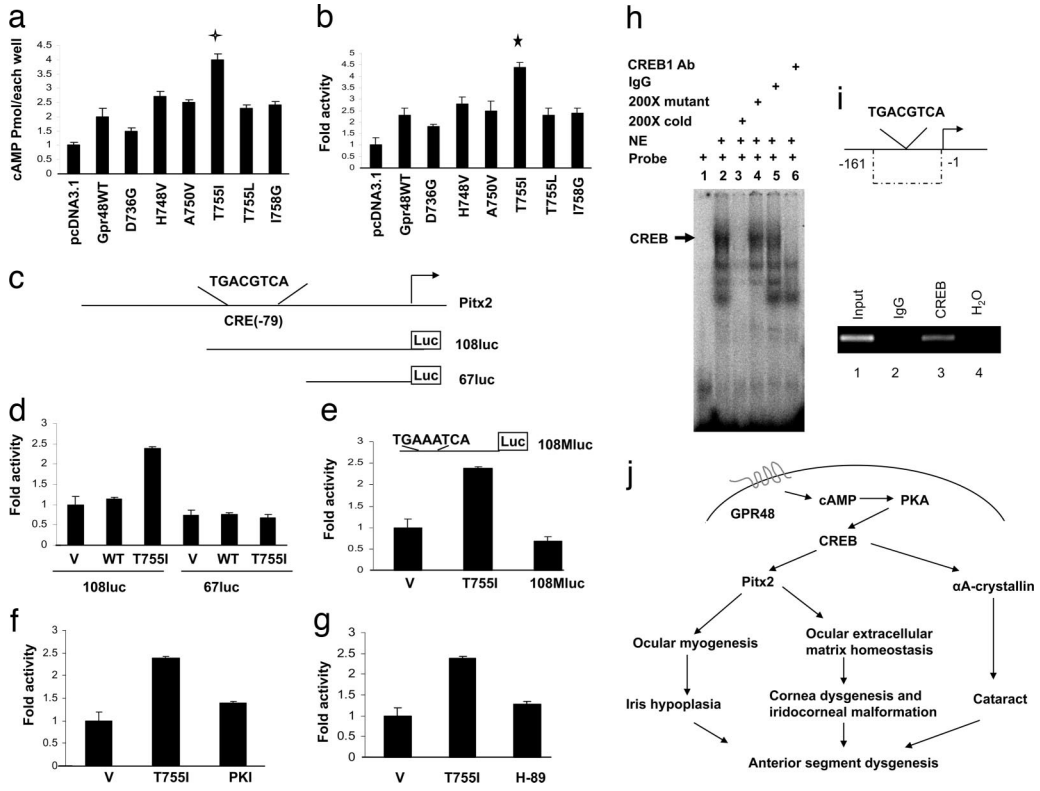

Fig. 4. Regulation of Pitx2 expression by Gpr48 through cAMP-PKA-CREB signaling pathway. (*a*) Activation of cAMP production by constitutively active Gpr48 mutant (T755I). (*b*) Activation of CRE luciferase reporter activity by Gpr48 T755I mutant receptor. (*c*) Diagram of the CRE-binding site in the *Pitx2* promoter and two Pitx2 luciferase reporters: luc-108, which contains the CRE site, and luc-67, which does not. (*d*) Activation of *Pitx2* 108-luc reporter by Gpr48 active mutant (T755I). *Pitx2* 67-luc reporter (no CRE-binding site) was not activated by the active mutant receptor. (*e*) Point mutation of the CRE site (from TGACGTCA to TGAAATCA) of the *Pitx2* promoter dramatically decreased the activation by Gpr48 active receptor (T755I). (*f* and *g*) PKI and H-89 inhibit the activation of the Pitx2 108-luc reporter mediated by the Gpr48 active receptor, respectively. (*h*) Binding of CREB transcription factor to the CRE-binding site of the *Pitx2* promoter region by EMSA assays. Lane 1, free probe; lane 2, nuclear extract from αT3–1 cells showing strong binding with *Pitx2* CRE probe; lane 3, 200-fold cold *Pitx2* CRE probe successfully shifted the binding; lane 4, 200-fold mutant *Pitx2* CRE probe failed to shift the band; lane 5, anti-IgG antibody did not shift the binding of the CRE probe; lane 6, anti-CREB antibody successfully shifted the binding complex of the *Pitx2* CRE probe. (*i*) ChIP assays of the CRE site in the *Pitx2* promoter demonstrate that anti-CREB antibody can successfully precipitate the DNA fragment in the promoter region of *Pitx2*. (*j*) Diagram of Gpr48 signaling pathways and regulation of ASD by Gpr48 through down-regulation of Pitx2 expression. Activation of Gpr48 leads to the production of intracellular cAMP and the activation of PKA. PKA can phosphorylate and regulate the activity of CREB, a key transcription factor that regulates the expression levels of many key genes, such as *Pitx2* and *αA-crystallin*, in anterior segment development and dysgenesis.

controls the expansion and constriction of iris pigment epithelial cells, so the proper amount of light can enter the eyes. Again, *Pitx2* was identified as one of the key genes regulating iris development (19). Down-regulation of Pitx2 leads to defects in iris development (20). In *Pitx2* heterozygous mice, the iris was hypoplastic, and the periocular muscle was diminished (13, 20).

In *Gpr48*$^{-/-}$ mice, keratopathy was frequently detected, indicating the protective function of the cornea epithelium, and the integrity of the cornea may be compromised. At early stages of eye development, we found that cornea epithelial cell proliferation and differentiation are dramatically decreased in *Gpr48*$^{-/-}$ mice, resulting in a thin and poorly developed cornea epithelium. The cornea contains a large number of extracellular matrix proteins important for cornea homeostasis. In *Gpr48*$^{-/-}$ mice, the expression levels of corneal extracellular matrix molecules, including collagen I, collagen V, BGN, OGN, keraton, Den, and lumican (21), are all decreased in *Gpr48*-null mutant mice. Collagen I and V provide the structural support for the cornea, whereas proteoglycans, including lumican, keratocan, OGN, Den, and BGN, function to coordinate the collagen fibril diameter and collagen fibril interspacing (22). Down-regulation of these molecules has been demonstrated to affect collagen structure, cornea clarity, and the homeostasis of corneal cells (23). Furthermore, we found that deletion of *Gpr48* significantly decreased the expression levels of two key enzymes, Plod1 and Plod2, that are responsible for hydroxylizing lysines in collagens through the down-regulation of Pitx2. It has been shown that both *PLOD1* and *PLOD2* promoters contain multiple PITX2-binding elements and are regulated by PITX2 in the pathology of Rieger syndrome (16), suggesting that PLOD1 and PLOD2 are indirect targets of GPR48 through PITX2.

In ≈26% (13/47) of *Gpr48*-null mutant mice, we detected lens opacity with abnormal large lens fiber cells and insoluble lens protein in the cells, indicating the occurrence of cataract. This phenotype is similar to αA-crystallin knockout mice, in which mutant mice develop lens cataract (24). In fact, the decreased soluble αA-crystallin protein level and increased insoluble αA-crystallin protein in *Gpr48*$^{-/-}$ mouse eyes indicate that Gpr48 is important for αA-crystallin stability in the lens. In *Gpr48*$^{-/-}$ mice <6 months of age, we did not detect any significant difference of the mutant retina from wild type. However, ganglion cell loss, inner nuclear layer thinness, and outer nuclear layer disorganization are frequently observed in *Gpr48*-null mice older than 6 months. Because ganglion cell loss and thinness of the inner nuclear cell layer are early indicators of glaucoma (19), our data suggest that Gpr48 could play an important role in the early onset of glaucoma and its development.

To understand the molecular mechanisms that mediate ASD in *Gpr48*$^{-/-}$ mice, we analyzed the expression levels of >20 different transcription factors and found that Pitx2 was significantly down-regulated in the *Gpr48*$^{-/-}$ mouse. *PITX2* is a homeodomain transcription factor implicated as the gene responsible for Atenfield–Rieger Syndrome (ARS) in humans (25). ARS is an autosomal dominant genetic disorder characterized by malformation of multiple tissues, including iris hypoplasia and iridogoniodysgenesis syndrome (15). Forty percent of patients diagnosed with classical ARS have *PITX2* mutations (26). Pitx2 is a key gene for mesenchymal epithelial transmission, regulating both craniofacial myogenesis and extracellular matrix synthesis in heart and cornea (20, 27). We identified and characterized the binding of the CREB transcription factor to a consensus CRE site at position −79 relative to the transcription start site of the *Pitx2* promoter using promoter

luciferase, EMSA, and ChIP assays. Therefore, our studies demonstrate that Gpr48 can regulate the expression level of Pitx2 through the cAMP-PKA-CREB pathway, and that the CRE-binding site at −79 in the promoter of *Pitx2* specifically mediates this activation. Although there is evidence that Pitx2 is partially controlled by the nodal signaling pathway (28), our studies provide strong evidence that GPCR and the G protein-mediated cAMP-PKA-CREB pathway can directly regulate the expression level of a key transcription factor Pitx2 during development, suggesting that Gpr48 may regulate eye and other organ development through the regulation of Pitx2.

To understand the signaling pathways mediated by Gpr48, we generated the ligand-independent constitutively active mutant receptor of Gpr48 (T755I). We demonstrate that this agonist-independent (constitutively) active mutant receptor can increase intracellular cAMP concentration and activate the intracellular cAMP-CREB signaling pathway. Receptors coupled to heterotrimeric GTP-binding proteins (G proteins) are integral membrane proteins and are targets for >50% of the pharmaceutical products sold in the world (29, 30). The study presented here suggests that Gpr48 is very important for anterior segment development of the eyes. Disruption of *Gpr48* causes ASD through down-regulation of the *Pitx2* gene, suggesting that Gpr48 could be a potential therapeutic target in the treatment of ASD.

Materials and Methods

Generation of *Gpr48* Gene Trap Mice. The *Gpr48* gene trap ES cell clone (LST020) was obtained from Williams Skarnes (Bay Genomics) (31, 32). The *Gpr48*-null ES cell clones were injected into C57BL/6 blastocysts and transferred to ICR females. Male chimera mice were mated with C57BL/6 females, resulting in transmission of the inserted allele to the germ line. Positive mice were interbred and maintained on a mixed 129 × C57BL/6 background.

Cell Proliferation and Apoptosis Assays. For PCNA staining, the Zymed PCNA Staining Kit (Zymed Laboratories) was used. For apoptosis assays, the ApopTag Plus Peroxidase In Situ Apoptosis Detection Kit from Chemicon was used. The pictures were captured on a CCD camera mounted on an inverted research microscope.

Mouse *Pitx2* Reporter Constructs. The mouse *Pitx2* proximal promoter region was obtained by PCR using mouse genomic DNA, then subcloned to $_p$GL3-Basic Vector (Promega). For generation of the point mutation of CREB binding on the promoter region, forward primer: F; 5′-GTGGAAT CTCTGC *TGAAATCA*CG AC ACTCC-3′ and reverse complement primer were used. All constructs encompassing the promoter region of mouse *Pitx2* were cloned into the promoterless pGL3 Basic Vector (Promega). The sequence of the constructs was verified by sequencing.

ChIP Assays. ChIP assays were performed as described (33). Briefly, αT3–1 cells were grown in 100-mm tissue culture plates, fixed with 1% formaldehyde, and lysed in SDS lysis buffer containing 1 mM phenylmethylsulfonyl fluoride, 1 μg/ml aprotinin, and 1 μg/ml pepstatin A. DNA was sheared to fragments of 200–500 bp by seven 10-s sonications. The chromatin was precleared with salmon sperm DNA/protein A-agarose slurry (Upstate Biotechnology) for 1 h at 4°C with gentle agitation. The agarose beads were pelleted, and the precleared supernatant was incubated with antibodies to CREB overnight at 4°C. The region between −161 and −1 of the *Pitx2* promoter was amplified from the immunoprecipitated chromatin by using the following primers: sense, 5′-TGATCGCCCAGCGTACAG-3′, and antisense, 5′-CTCGGTCTCGCACTCTCTCT-3′.

Data Analysis. All experimental data are presented as the mean ± SEM. Statistical significance was determined by the Mann–Whitney *U* test and Student's *t* test. Significance was accepted at $P < 0.05$.

ACKNOWLEDGMENTS. This work was partially supported by National Institutes of Health Grants 5R01HL064792 and 1R01CA106479 (to M.L.) and was also in part supported by grants from the National Natural Science Foundation of China (30771067) and the Zhejiang Provincial Natural Science Foundation of China (Z206842) (to L.T.). The *Gpr48* gene trap ES cell clone (LST020) was obtained from Bay Genomics at Mutant Mouse Regional Resource Centers of the University of California, Davis.

1. Puls A, *et al*. (1999) Activation of the small GTPase Cdc42 by the inflammatory cytokines TNF(alpha) and IL-1, and by the Epstein–Barr virus transforming protein LMP1. *J Cell Sci* 112:2983–2992.
2. Gould DB, John SW (2002) Anterior segment dysgenesis and the developmental glaucomas are complex traits. *Hum Mol Genet* 11:1185–1193.
3. Quigley HA, Broman AT (2006) The number of people with glaucoma worldwide in 2010 and 2020. *Br J Ophthalmol* 90:262–267.
4. Hsu SY, Liang SG, Hsueh AJ (1998) Characterization of two LGR genes homologous to gonadotropin and thyrotropin receptors with extracellular leucine-rich repeats and a G protein-coupled, seven-transmembrane region. *Mol Endocrinol* 12:1830–1845.
5. Loh ED, *et al*. (2000) Chromosomal localization of GPR48, a novel glycoprotein hormone receptor like GPCR, in human and mouse with radiation hybrid and interspecific backcross mapping. *Cytogenet Cell Genet* 89:2–5.
6. Loh ED, Broussard SR, Kolakowski LF (2001) Molecular characterization of a novel glycoprotein hormone G protein-coupled receptor. *Biochem Biophys Res Commun* 282:757–764.
7. Hsu SY, *et al*. (2000) The three subfamilies of leucine-rich repeat-containing G protein-coupled receptors (LGR): identification of LGR6 and LGR7 and the signaling mechanism for LGR7. *Mol Endocrinol* 14:1257–1271.
8. Van Schoore G, Mendive F, Pochet R, Vassart G (2005) Expression pattern of the orphan receptor LGR4/GPR48 gene in the mouse. *Histochem Cell Biol* 124:35–50.
9. Mazerbourg S, *et al*. (2004) Leucine-rich repeat-containing, G protein-coupled receptor 4 null mice exhibit intrauterine growth retardation associated with embryonic and perinatal lethality. *Mol Endocrinol* 18:2241–2254.
10. Mendive F, *et al*. (2006) Defective postnatal development of the male reproductive tract in LGR4 knockout mice. *Dev Biol* 290:421–434.
11. Hoshii T, *et al*. (2007) LGR4 Regulates the Postnatal Development and Integrity of Male Reproductive Tracts in Mice. *Biol Reprod* 76:303–313.
12. Gao Y, *et al*. (2006) Up-regulation of GPR48 induced by down-regulation of p27Kip1 enhances carcinoma cell invasiveness and metastasis. *Cancer Res* 66:11623–11631.
13. Lu MF, Pressman C, Dyer R, Johnson RL, Martin JF (1999) Function of Rieger syndrome gene in left-right asymmetry and craniofacial development. *Nature* 401:276–278.
14. Amendt BA, Sutherland LB, Semina EV, Russo AF (1998) The molecular basis of Rieger syndrome. Analysis of Pitx2 homeodomain protein activities. *J Biol Chem* 273:20066–20072.
15. Amendt BA, Semina EV, Alward WL (2000) Rieger syndrome: a clinical, molecular, and biochemical analysis. *Cell Mol Life Sci* 57:1652–1666.
16. Hjalt TA, Amendt BA, Murray JC (2001) PITX2 regulates procollagen lysyl hydroxylase (PLOD) gene expression: implications for the pathology of Rieger syndrome. *J Cell Biol* 152:545–552.
17. Gao Y, *et al*. (2006) Generation of a constitutively active mutant of human GPR48/LGR4, a G-protein-coupled receptor. *Hokkaido Igaku Zasshi* 81:101–105, 107:109.
18. Traboulsi EI (1998) Ocular malformations and developmental genes. *J Aapos* 2:317–323.
19. Gould DB, Smith RS, John SW (2004) Anterior segment development relevant to glaucoma. *Int J Dev Biol* 48:1015–1029.
20. Diehl AG, *et al*. (2006) Extraocular muscle morphogenesis and gene expression are regulated by Pitx2 gene dose. *Invest Ophthalmol Vis Sci* 47:1785–1793.
21. Meek KM, Boote C (2004) The organization of collagen in the corneal stroma. *Exp Eye Res* 78:503–512.
22. Chakravarti S (2002) Functions of lumican and fibromodulin: lessons from knockout mice. *Glycoconj J* 19:287–293.
23. Kao WW, Liu CY (2002) Roles of lumican and keratocan on corneal transparency. *Glycoconj J* 19:275–285.
24. Lang RA (2004) Pathways regulating lens induction in the mouse. *Int J Dev Biol* 48:783–791.
25. Alward WL (2000) Axenfeld-Rieger syndrome in the age of molecular genetics. *Am J Ophthalmol* 130:107–115.
26. Lines MA, Kozlowski K, Walter MA (2002) Molecular genetics of Axenfeld-Rieger malformations. *Hum Mol Genet* 11:1177–1184.
27. Dagle JM, *et al*. (2003) Pitx2c attenuation results in cardiac defects and abnormalities of intestinal orientation in developing *Xenopus laevis*. *Dev Biol* 262:268–281.
28. Duboc V, Lepage T (2008) A conserved role for the nodal signaling pathway in the establishment of dorso-ventral and left-right axes in deuterostomes. *J Exp Zool* 310:41–53.
29. Howard AD, *et al*. (2001) Orphan G-protein-coupled receptors and natural ligand discovery. *Trends Pharmacol Sci* 22:132–140.
30. Bai M (2004) Dimerization of G-protein-coupled receptors: Roles in signal transduction. *Cell Signal* 16:175–186.
31. Stryke D, *et al*. (2003) BayGenomics: A resource for gene-trapped mouse embryonic stem cells. *Nucleic Acids Res* 31:278–281.
32. Skarnes WC, *et al*. (2004) A public gene trap resource for mouse functional genomics. *Nat Genet* 36:543–544.
33. Mitchell DC, Stafford LJ, Li D, Bar-Eli M, Liu M (2006) Transcriptional regulation of KiSS-1 gene expression in metastatic melanoma by specificity protein-1 and its coactivator DRIP-130. *Oncogene* 26:1739–1747.